Biochemistry

 Volume 42, Number 27 July 15, 2003

Accelerated Publications

Unlocking the Molecular Structure of Fungal Melanin Using ^{13}C Biosynthetic Labeling and Solid-State NMR†

Shiying Tian,‡ Javier Garcia-Rivera,§ Bin Yan,‡ Arturo Casadevall,§ and Ruth E. Stark*,‡

Department of Chemistry, City University of New York Graduate Center and College of Staten Island, Staten Island, New York 10314-6600, and Department of Immunology, Albert Einstein College of Medicine, Yeshiva University, Bronx, New York 10461

Received February 3, 2003; Revised Manuscript Received May 23, 2003

ABSTRACT: Melanins are enigmatic pigments found in all biological kingdoms that are associated with a variety of functions, including microbial virulence. Despite being ubiquitous in nature, melanin pigments have long resisted atomic-level structural examination because of their insolubility and amorphous organization. *Cryptococcus neoformans* is a human pathogenic fungus that melanizes only when provided with exogenous substrate, thus offering a unique system for exploring questions related to melanin structure at the molecular level. We have exploited the requirement for exogenous substrate in melanin synthesis as well as the capabilities of high-resolution solid-state nuclear magnetic resonance (NMR) to establish the predominantly aliphatic composition of L-dopa melanin and to introduce ^{13}C labels that permit the identification of proximal carbons in the developing biopolymer. By swelling solid melanin samples in organic solvents and using two-dimensional heteronuclear NMR in conjunction with magic-angle spinning, we have identified chemical bonding patterns typical of alkane, alkene, alcohol, ketone, ester, and indole functional groups. These findings demonstrate the feasibility of a novel approach to determining the structure of melanin using metabolic labeling and NMR spectroscopy.

Melanins make up a heterogeneous class of natural pigments that have a myriad of biological functions, including protection against sunlight, energy transduction, and camouflage (*1*). Melanins are found in bacteria, fungi, plants, and animals; they are believed to be composed of polymerized phenolic or indolic compounds that are highly resistant to degradation (*2*). Melanin is believed to be responsible for the remarkable resistance of human melanoma cells to therapeutic radiation and chemotherapy (*3*, *4*). In several opportunistic pathogenic fungi, including *Cryptococcus neoformans*, melanin synthesis is associated with virulence. Despite their biological importance, natural melanins have defied chemical and structural analysis; these materials are amorphous, heterogeneous, insoluble, and resistant to crystallization. For instance, the insolubility of brown or black nitrogen-containing eumelanins precludes their study with solution-state hydrodynamic, spectroscopic, and light scattering techniques. Similarly, their amorphous character makes it impossible to determine their molecular structures using current crystallographic techniques. Hence, a full accounting of the melanin structure remains beyond our current analytical horizon.

† A.C. and R.E.S. gratefully acknowledge support from NIH Grant AI052733; R.E.S. also acknowledges support from NSF Grants MCB/IBN 9728503 and MCB 0134705. R.E.S. is a Principal Investigator of the New York Structural Biology Center.

* To whom correspondence should be addressed. E-mail: stark@mail.csi.cuny.edu.

‡ City University of New York Graduate Center and College of Staten Island.

§ Yeshiva University.

10.1021/bi0341859 CCC: $25.00
Published on Web 06/19/2003

To meet these investigative challenges, several research groups have used high-resolution ^{13}C and ^{15}N solid-state NMR[1] in conjunction with established chemical shift trends to tentatively identify functional groups in synthetic and natural eumelanins from animal or fungal sources (*5*−*9*). Although signals from carboxylic acids, aromatics, and uncyclized aliphatic chains have been found in all of these materials, their relative spectral intensities vary widely due to the diverse sample sources and the possible presence of proteinaceous contaminants (*7*). Broad line widths have been attributed to the structural heterogeneity of each biopolymer as well as the presence of paramagnetic centers (*10*). These approaches provide tantalizing first looks at the structural features of such intractable materials, but they are limited by uncertainties in both the numerical values and interpretations of the chemical shifts. Alternatively, solution-state NMR has been used for more than two decades to characterize melanins and soil organic matter dissolved in a strong base (*5*, *11*−*14*). As with chemical degradation methods, an incomplete or distorted picture of the original material may result from this procedure, and in practice, the ^{13}C and ^{1}H spectra have often displayed disappointing resolution attributed to high viscosity, unpaired electron density, and chemical heterogeneity.

In contrast to many other microorganisms, *C. neoformans* synthesizes melanin only in the presence of exogenous substrates, namely, *o*-diphenols such as L-dopa (L-3,4-dihydroxyphenylalanine) that have hydroxyl groups at positions 2 and 3 or 3 and 4 of the phenyl group (*15*). The pigment is deposited in the cell wall and can be extracted in the form of hollow particles that resemble cells (melanin "ghosts") using denaturants and hot HCl (*16*). Since melanin synthesis in *C. neoformans* is completely dependent upon exogenous substrate, it is possible to obtain a biopolymer derived from a single precursor that can be labeled isotopically. In the current work, we have used ^{13}C-labeled L-dopa to biosynthetically label particular melanin sites; their signals dominate the solid-state ^{13}C NMR spectra and illustrate how proximal carbons in the biopolymer structure may be identified. Furthermore, we have been able to achieve liquid-like spectral resolution simply by swelling insoluble fungal melanin in appropriate solvents and acquiring the NMR spectra under magic-angle spinning (MAS) conditions. This approach was validated previously for synthetic polymer gels (*17*) and extended to multidimensional spectroscopy of natural plant polymers (*18*−*20*). The combination of ^{13}C biosynthetic labeling, solid-state NMR, and sample swelling has allowed us to identify key functional groups in *C. neoformans* melanin and suggests a general strategy for more comprehensive elucidation of the molecular structure of this enigmatic polymer.

MATERIALS AND METHODS

C. neoformans Melanin. Melanin particles from melanized *C. neoformans* cells were prepared as described previously (*21*). For isotopically enriched samples, 2,3-$^{13}C_2$(97%),4-^{18}OH(95%)-L-dopa was obtained from Cambridge Isotope Laboratories.

NMR Measurements. Data were obtained on Varian (Palo Alto, CA) UNITY*plus* 300 widebore and ^{UNITY}INOVA 600 NMR spectrometers located at City University of New York College of Staten Island. For solid-state ^{13}C experiments, 10−30 mg samples were spun at a typical speed of 9.00 ± 0.01 kHz in a 5 mm probe from Doty Scientific (Columbia, SC). For swelled-solid experiments, 7 mg of melanin was equilibrated in 35 mg of DMSO-d_6 and the mixture spun typically at 2.500 ± 0.001 kHz in a Varian 40 μL ^{1}H-optimized nanoprobe using 11 G/cm pulsed field gradients.

Cross-polarization magic-angle spinning (CPMAS) ^{13}C experiments were conducted with a ^{1}H decoupling strength of 50 kHz, a delay time of 1 s between successive acquisitions, a line broadening of 50−100 Hz, and contact times of 0.5−2.5 ms to establish the ratios of rigid carbon moieties (*22*). Direct polarization MAS ^{13}C experiments were carried out with 6 and 50 kHz of ^{1}H decoupling during the signal acquisition period, to estimate the proportions of mobile and rigid methylene groups, respectively. Delayed decoupling experiments were performed with 60 μs of dipolar dephasing to remove signals from rigid protonated carbons (*23*). Two-dimensional $^{13}C-^{13}C$ spin-exchange experiments were conducted with mixing times of 0.01−2.0 s as described previously (*24*). Chemical shifts are quoted with respect to tetramethylsilane via hexamethylbenzene as a secondary substitution reference.

MAS ^{1}H experiments with solvent-swelled samples included one-pulse spectral acquisitions as well as two-dimensional $^{1}H-^{13}C$ gradient-assisted heteronuclear multiple-quantum coherence (gHMQC) (*25*) and heteronuclear multiple-bond correlation (gHMBC) (*26*) experiments implemented by adding rotor synchronization to published pulse sequences. ^{1}H and ^{13}C chemical shifts were referenced to DMSO at 2.49 and 39.5 ppm, respectively.

RESULTS AND DISCUSSION

Compositional and Dynamic Profiles of Fungal Melanin from Solid-State ^{13}C NMR. A comparison of CPMAS ^{13}C NMR spectra for melanins from several fungal sources is shown in Figure 1. In all cases, the chemical shifts were consistent with molecular structures that include open chain methylene groups (30 ppm), oxygenated aliphatic carbons (72 ppm), aromatic and/or olefinic carbons (110−160 ppm), and carboxyls (170 ppm). There were no prominent spectral features that could be attributed to proteinaceous materials (C_α, ~50 ppm) or phenolic moieties (58 and 150 ppm); the peak at 72 ppm may include contributions from polysaccharides in the fungal cell wall. The signal intensities measured as a function of cross-polarization time (data not shown) verify that this spectrum provides a fair compositional estimate of the rigid carbons in the melanin sample. Although differing experimental parameters and preparation histories limit the reliability of comparisons among the different samples, the molecular composition of L-dopa melanin from *C. neoformans* ghost preparations was nevertheless striking in its preponderance of bulk methylenes and the paucity of unsaturated residues. This compositional finding was unexpected in light of the prevailing view that melanin synthesis proceeds by polymerization of intact aromatic rings (*15*). Significant spectroscopic variations among the pigments from different fungal sources, which have been noted previously (*13*), suggest that the word "melanin" should refer to a class

[1] Abbreviations: NMR, nuclear magnetic resonance; MAS, magic-angle spinning; CPMAS, cross-polarization magic-angle spinning; HMQC, heteronuclear multiple-quantum coherence; HMBC, heteronuclear multiple-bond correlation.

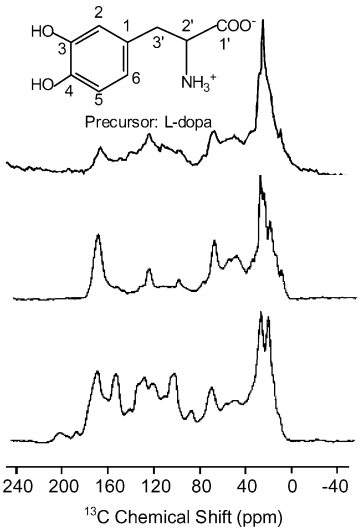

FIGURE 1: CPMAS ^{13}C NMR spectra of solid fungal melanins: 25 MHz spectrum of *Oidiodendron tenuissimum* melanin, adapted from ref *8* (bottom), 25 MHz spectrum of *Trichoderma harzianum* melanin, adapted from ref *8* (middle), and 75 MHz spectrum of *C. neoformans* melanin, produced with a natural-abundance L-dopa precursor (shown above the spectrum) and requiring 9 h of spectral acquisition (top).

of materials with similar physical properties but possibly different molecular structures.

Additional insight into the molecular architecture of this melanin was gained from MAS ^{13}C NMR spectra obtained without cross-polarization or nuclear Overhauser effects. By comparison of the integrated peak intensities with and without high-power decoupling (data not shown), it is estimated that 35% of the methylene chain segments undergo sufficient motion at 75 MHz to exhibit liquid-like spectra. Significant molecular mobility of these chains is also evident from the retention of some methylene chain NMR signals under delayed decoupling conditions and the observation of 5 kHz ^1H CH_2 line widths in wide-line separation experiments. Although somewhat surprising in light of melanin's insolubility in organic and aqueous solvents, this finding of molecular flexibility has precedent in studies of an intractable protective polymer in the skin of plants (*27*).

Other than in the chain methylene region, the spectral lines are broader than those observed in some fungal melanins (*8*) but better resolved than those for melanins from animal and synthetic sources (*6*, *7*). These trends may reflect variations in chemical heterogeneity and/or unpaired electron content. Significant narrowing of most *C. neoformans* melanin spectral lines occurred upon exposure of the dry samples to D_2O (data not shown), indicating motional narrowing, diminution of $^{13}C-^1H$ dipolar interactions due to exchange of deuterons for protons, or both phenomena. Since the same narrowing effect is observed in H_2O and with extended exposure to D_2O, it is possible to rule out chemical exchange in this biopolymer system.

Site-Specific Incorporation of ^{13}C Labels and Structural Information. As noted above, *C. neoformans* requires exogenous substrates to synthesize melanin. This requirement allows the investigator to choose the substrate and isotopic labeling pattern to probe particular structural elements spectroscopically and to monitor the consequences of biosynthetic incorporation into the developing polymer. Figure

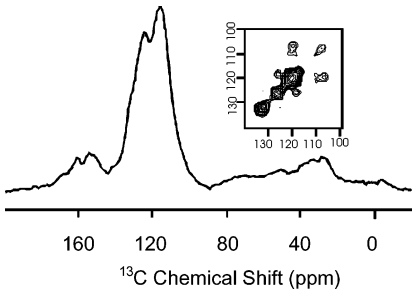

FIGURE 2: CPMAS ^{13}C NMR spectrum (75 MHz) of *C. neoformans* melanin produced with a 2,3-$^{13}C_2$-L-dopa substrate. The inset shows a contour plot from a 14 h 2D proton-driven $^{13}C-^{13}C$ spin diffusion experiment on the selectively ^{13}C-enriched melanin sample.

2 shows CPMAS ^{13}C NMR results for *C. neoformans* melanin synthesized in the presence of a 2,3-$^{13}C_2$-L-dopa substrate, in which resonances corresponding to the two enriched protonated aromatic carbons are dramatically enhanced compared with the chain methylenes, but some ^{13}C incorporation may also occur for resonances at 30 and 150 ppm. If the amount of aliphatic signal in Figure 1 (top) is assumed provisionally to be unchanged in the spectrum of Figure 2, then the integrated intensity of the aromatic spectral region is found to increase 9-fold.

The ability to observe prominent aromatic resonances in the ^{13}C-labeled sample (Figure 2) suggests that the modest signal intensity evident in the natural-abundance sample can be attributed to a small proportion of this carbon type in *C. neoformans* melanin rather than an effect of paramagnetic broadening. Although the resonance at 124 ppm exhibits a chemical shift comparable to position 2 in the L-dopa monomer (*6*), the peak at 114 ppm varies significantly from monomer position 3 (145 ppm), suggesting that the latter site is no longer occupied by a hydroxyl group upon formation of the biopolymer.

With the incorporation of ^{13}C-enriched substrates into *C. neoformans* melanin, it also becomes possible to test hypotheses regarding the spatial proximity and covalent bonding of particular molecular sites. As an illustration, the inset of Figure 2 shows results from a $^{13}C-^{13}C$ spin diffusion experiment on this material. The observation of strong cross-peaks demonstrates the proximity of the labeled carbons, in accord with prior reports which showed that these directly bound atoms in L-dopa remain covalently linked in the melanin polymer (*28*). However, preliminary comparison of the normalized cross-peak intensities with analogous results for ring-labeled phenylalanine (not shown) suggests that only half of the carbon pairs remain neighbors during melanin biosynthesis.

Molecular Structures from NMR of Swelled Melanin Samples. As noted above, MAS ^{13}C NMR indicated a surprisingly significant degree of motional averaging in unlabeled powdered melanin. In addition, the spectral narrowing evidenced for many of the resonances upon exposure to D_2O and H_2O suggested that the biopolymer could be swelled readily in common solvents. These observations prompted us to collect high-sensitivity MAS ^1H NMR spectra under solvent-swelled conditions, exploiting the fact that this protocol simultaneously enhances molecular mobility and minimizes magnetic susceptibility line broadening (*29*, *30*). Figure 3 displays a typical 600 MHz NMR spectrum of *C. neoformans* melanin swelled in DMSO.

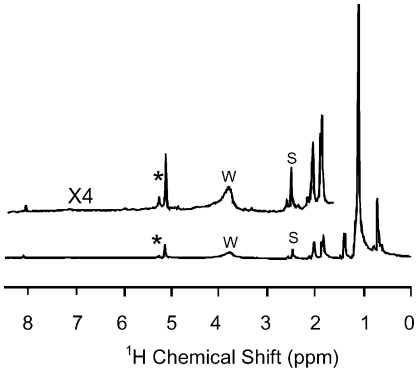

FIGURE 3: MAS ^{1}H NMR spectrum (600 MHz) of *C. neoformans* melanin, swelled at 1:5 (w/w) in DMSO-d_6 at 25 °C and spun at 2.5 kHz. Peaks from the DMSO and water are labeled s and w, respectively; a spinning sideband is marked with an asterisk. An additional peak at 3.83 ppm is visible if the sample is swelled in D_2O.

Even at modest spinning speeds of 2−3 kHz, the one-dimensional (1D) spectra exhibit flat baselines and reasonably narrow lines; the 20−25 Hz line widths preclude the observation of *J* couplings but are comparable to those exhibited by neuromelanins dissolved in a strong base (*14*) and to those of swelled samples of plant biopolyesters (*19*, *20*). Similar spectral features are observed at temperatures from 20 to 50 °C or if the swelling is done with D_2O. The integrated intensities of the various ^{1}H resonances confirmed the predominance of methylene and other aliphatic groups, as deduced independently from ^{13}C CPMAS and direct polarization MAS of dry melanin (*vide supra*). Also notable is a small resonance at 8.10 ppm, attributed provisionally to the pyrrole CH group of a carboxyl-substituted indole (*31*). Finally, a secondary alcohol peak (3.83 ppm) is visible when the sample is swelled in D_2O, though it is partially obscured by the residual H_2O signal when the sample is swelled in DMSO. The overall concordance of compositional profiles derived from solid-state and swelled-solid NMR added a measure of confidence to the quantitative reliability of both methodologies. Nevertheless, the paucity of ^{1}H signals from multiply bonded moieties may indicate incomplete accessibility to solvent, and complications from paramagnetic broadening cannot be ruled out for either type of NMR data.

To identify functional groups definitively, the MAS-assisted NMR approach was also used to obtain two-dimensional heteronuclear correlated spectra of fungal melanin swelled in DMSO, as shown in Figures 4 and 5. The ^{13}C HMQC spectrum (Figure 4) separates overlapping ^{1}H NMR signals according to the different resonance positions of their attached ^{13}C nuclei, identifies directly bonded hydrogen−carbon pairs, and serves as a fingerprint of the hydrogen- and carbon-containing functional groups present in the biopolymer (*25*). With the benefit of correlated ^{1}H and ^{13}C chemical shifts, it was possible to confirm the likely presence in fungal melanin of methyl groups ($\underline{CH_3}CH_2$, 0.74 and 13.8 ppm; $\underline{CH_3}COO$, 2.05 and 33.7 ppm), several environmentally distinct types of long chain methylenes (e.g., 1.13 with 22.4, 29.4, and 31.8 ppm), proton-bearing carbons attached and adjacent to double bonds ($\underline{CH}$═CH, 5.16 and 129.6 ppm; $\underline{CH_2}CH$═CH, 1.86 and 26.9 ppm), and methylenes near carbonyls ($\underline{CH_2}COO$, 1.89 and 21.1 ppm; $\underline{CH_2}$-C═O, 2.06 and 30.0 ppm). A cross-peak at 3.83 and 63.4 ppm, consistent with a secondary alcohol group, is also identified tentatively near the signal from residual water in the DMSO solvent (data not shown). The carbon shifts are in satisfactory agreement with the CPMAS ^{13}C data presented above; the narrow line widths of these two-dimensional (2D) spectra make it possible, moreover, to discriminate among environmentally similar protons and carbons as is done routinely for organic molecules in solution (*32*).

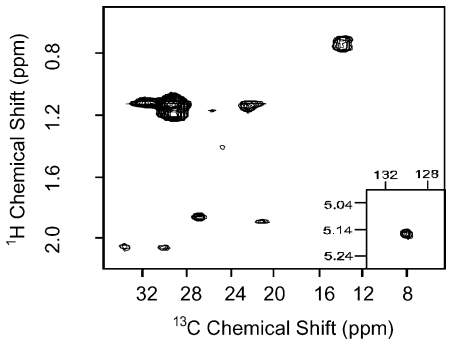

FIGURE 4: Contour plot of single-bond correlations from a gradient-assisted 2D ^{1}H−^{13}C HMQC NMR experiment on *C. neoformans* melanin, conducted with 2.5 kHz magic-angle spinning and *z*-axis pulsed field gradients. Regions corresponding to aliphatic chain methylene, methyl, and alkene groups are shown; an additional cross-peak that can be attributed to a secondary alcohol group is also visible near the signal from residual water present in the DMSO solvent.

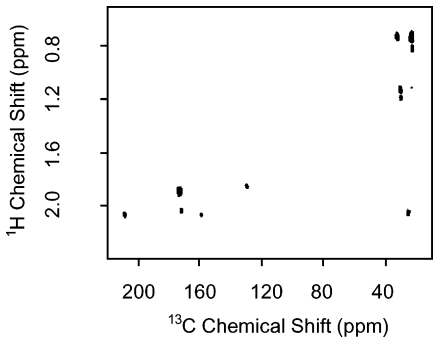

FIGURE 5: Contour plot of long-range through-bond correlations from a gradient-assisted 2D ^{1}H−^{13}C HMBC NMR experiment on *C. neoformans* melanin, conducted as described in the legend of Figure 4. No other cross-peaks appeared in the spectrum.

Finally, Figure 5 shows a ^{13}C HMBC spectrum for swelled fungal melanin under MAS NMR conditions. This experiment reveals long-range covalent connectivities involving nonprotonated carbons that are not reported in HMQC spectra; it also displays cross-peaks that confirm the presence of functional groups proposed above: ketones ($C\underline{H_2}C$═O, 2.06 and 208.7 ppm), esters ($C\underline{H_2}COO$, 1.89 and 173.5 ppm; $C\underline{H_3}COO$, 2.05 and 172.1 ppm), and olefins ($C\underline{H_2}H\underline{C}$═CH, 1.86 and 129.6 ppm). The long-range coupling shown by the cross-peak at 2.06 and 158.8 ppm may be attributed to an aromatic-linked carboxylate moiety (*5*). These observations extend the structural information deduced from CP-MAS, 1D, and HMQC experiments to yield definitive evidence for previously unknown fragments in the molecular structure of this fungal melanin.

Implications for Elucidation of Melanin Molecular Structure and Development. By exploiting the capabilities of both solid- and solution-state NMR and the unique requirement of *C. neoformans* melanin for exogenous substrates, we obtained significant new structural information for this enigmatic biopolymer. The molecular composition of this

melanin is predominantly aliphatic, including uncyclized methylene groups that exhibit a high degree of flexibility. Many aromatic linkages such as the C2−C3 bond in L-dopa are retained when this substrate is incorporated into the developing pigment, though the chemistry by which the aliphatic moieties are synthesized requires further investigation. Molecular motion is enhanced throughout the polymeric structure upon swelling in solvents such as H_2O or DMSO, making it possible to obtain high-resolution ^1H NMR spectra and identify $^1H-^{13}C$ pairs that are directly or remotely bonded within the melanin structure. By augmenting the tentative structural assignments made traditionally from ^{13}C chemical shift trends, we were able to identify functional groups such as alkanes, alkenes, alcohols, ketones, and carboxylic acid esters. The resulting preliminary picture of melanin's molecular architecture is nevertheless more definitive and more comprehensive than that established previously by elemental analysis and magnetic resonance spectroscopies.

Among the great pigments of nature, the melanins are the least understood because their structures are undetermined. The foregoing studies demonstrate both the feasibility and future promise of NMR spectroscopy for building a comprehensive molecular picture of melanin. A variety of substrates may be used in biosynthetic labeling experiments, and covalent connections between the structural moieties may be identified by a suitable choice of isotopic labels and NMR experiments. These strategies offer the exciting prospect of identifying complex nitrogen-containing aromatic ring structures, uncyclized aliphatic chains, and possible melanin−polysaccharide linkages that underlie the function of this important biological material.

ACKNOWLEDGMENT

We thank Dr. Hsin Wang for assistance with the NMR experiments.

REFERENCES

1. Hill, H. Z. (1992) The function of melanin or six blind people examine an elephant, *BioEssays 14*, 49−56.
2. Henson, J. M., Butler, M. J., and Day, A. W. (1999) The dark side of the mycelium: melanins of phytopathogenic fungi, *Annu. Rev. Phytopathol. 37*, 447−471.
3. Schwabe, K., Lassmann, G., Damerau, W., and Naundorf, H. J. (1989) Protection of melanoma cells against superoxide radicals by melanins, *Cancer Res. Clin. Oncol. 115*, 597−600.
4. Kinnaert, E., Morandini, R., Simon, S., Hill, H. Z., Ghanem, G., and Van Houtte, P. (2000) The degree of pigmentation modulates the radiosensitivity of human melanoma cells, *Radiat. Res. 154*, 497−502.
5. Schnitzer, M., and Chan, Y. K. (1983) Structural characteristics of a fungal melanin and a soil humic acid, *Soil Sci. Soc. Am. J. 50*, 67−71.
6. Duff, G. A., Roberts, J. E., and Foster, N. (1988) Analysis of the structure of synthetic and natural melanins by solid-phase NMR, *Biochemistry 27*, 7112−7116.
7. Hervé, M., Hirschinger, J., Granger, P., Gilard, P., Deflandre, A., and Goetz, N. (1994) A ^{13}C solid-state NMR study of the structure and auto-oxidation process of natural and synthetic melanins, *Biochim. Biophys. Acta 1204*, 19−27.
8. Knicker, H., Almendros, G., González-Vila, F. J., Lüdemann, H.-D., and Martin, F. (1995) ^{13}C and ^{15}N NMR analysis of some fungal melanins in comparison with soil organic matter, *Org. Geochem. 23*, 1023−1028.
9. Aime, S., Fasano, M., Bergamasco, B., Lopiano, L., and Quattrocolo, G. (1996) Nuclear magnetic resonance spectroscopy characterization and iron content determination of human mesencephalic neuromelanin, in *Advances in Neurology* (Battistini, L., Scarlato, G., Caraceni, T., and Ruggieri, S., Eds.) pp 263−270, Lippincott-Raven Publishers, Philadelphia.
10. Felix, C. C., Hyde, J. S., Sarna, T., and Sealy, R. C. (1978) Interactions of melanin with metal ions. Electron spin resonance evidence for chelate complexes of metal ions with free radicals, *J. Am. Chem. Soc. 100*, 3922−3926.
11. Gonzalez-Vila, F. J., Martin, F., and Saiz-Jimenez, C. (1978) C-13 Nuclear magnetic resonance spectra of soil humic fractions and fungal melanins, *Agrochimica 22*, 501−505.
12. Gonzalez-Vila, F. J., Saiz-Jimenez, C., Lentz, H., and Lüdemann, H.-D. (1978) ^{13}C nuclear magnetic resonance spectra of fungal melanins, *Z. Naturforsch. 33c*, 291−293.
13. Lüdemann, H. D., Lentz, H., and Martin, J. P. (1982) Carbon-13 Nuclear magnetic resonance spectra of some fungal melanins and humic acids, *Soil Sci. Soc. Am. J. 46*, 957−962.
14. Double, K. L., et al. (2000) Structural characteristics of human substantia nigra neuromelanin and synthetic dopamine melanins, *J. Neurochem. 75*, 2583−2589.
15. Chaskes, S., and Tyndall, R. L. (1975) Pigment production by *Cryptococcus neoformans* from *para*- and *ortho*-diphenols: effect of the nitrogen source, *J. Clin. Microbiol. 1*, 509−514.
16. Wang, Y., Aisen, P., and Casadevall, A. (1996) Melanin, melanin "ghosts," and melanin composition in *Cryptococcus neoformans*, *Infect. Immun. 64*, 2420−2424.
17. Stöver, H. D. H., and Fréchet, J. M. J. (1991) NMR characterization of crosslinked polystyrene gels, *Macromolecules 24*, 883−888.
18. Gil, A. M., Lopes, M. H., Neto, C. P., and Rocha, J. (1999) Very high-resolution ^1H MAS NMR of a natural polymeric material, *Solid State NMR 15*, 59−67.
19. Stark, R. E., Yan, B., Ray, A. K., Chen, Z., Fang, X., and Garbow, J. R. (2000) NMR studies of structure and dynamics in fruit cuticle polyesters, *Solid State NMR 16*, 37−45.
20. Fang, X., Qiu, F., Yan, B., Wang, H., Mort, A. J., and Stark, R. E. (2001) NMR Studies of Molecular Structure in Fruit Cuticle Polyesters, *Phytochemistry 57*, 1035−1042.
21. Rosas, A. L., Nosanchuk, J. D., Gomez, B. L., Edens, W. A., Henson, J. M., and Casadevall, A. (2000) Isolation and serological analyses of fungal melanins, *J. Immunol. Methods 244*, 69−80.
22. Schaefer, J., and Stekskal, E. O. (1979) High-resolution ^{13}C NMR of solid polymers, *Top. Carbon-13 NMR Spectrosc. 3*, 283−324.
23. Opella, S. J., Frey, M. H., and Cross, T. A. (1979) Selection of nonprotonated carbon resonances in solid-state nuclear magnetic resonance, *J. Am. Chem. Soc. 101*, 5854−5857.
24. Yan, B., and Stark, R. E. (2000) Biosynthesis, molecular structure and domain architecture of potato suberin: A solid-state ^{13}C NMR study using ^{13}C-enriched precursors, *J. Agric. Food Chem. 48*, 3298−3304.
25. Hurd, R. E., and John, B. K. (1991) Gradient enhanced proton-detected heteronuclear multiple-quantum coherence spectroscopy, *J. Magn. Reson. 91*, 648−653.
26. Rinaldi, P. L., and Keifer, P. A. (1994) The utility of pulsed-field-gradient HMBC for organic structure determination, *J. Magn. Reson., Ser. A 108*, 259−262.
27. Garbow, J. R., and Stark, R. E. (1990) Nuclear magnetic resonance relaxation studies of plant polyester dynamics. 1. cutin from limes, *Macromolecules 23*, 2814−2819.
28. Williamson, P. R., Wakamatsu, K., and Ito, S. (1998**)** Melanin biosynthesis in *Cryptococcus neoformans*, *J. Bacteriol. 180*, 1570−1572.
29. Keifer, P. A., Balthusis, L., Rice, D. M., Tymiak, A. A., and Shoolery, J. N. (1996) A comparison of NMR spectra obtained for solid-phase-synthesis resins using conventional high-resolution, magic-angle-spinning, and high-resolution magic-angle-spinning probes, *J. Magn. Reson., Ser. A 119*, 65−75.
30. Millis, K., Maas, W. E., Singer, S., and Cory, D. G. (1997) Gradient, high-resolution, magic-angle spinning nuclear magnetic resonance spectroscopy of human adipocyte tissue, *Magn. Reson. Med. 38*, 399−403.
31. ACD/CNMR Spectrum Generator (2000) Advanced Chemistry Development, Toronto, ON.
32. Martin, G. E., and Zektzer, A. S. (1988) *Two-Dimensional NMR Methods for Establishing Molecular Connectivity*, VCH Publishers, New York.

BI0341859